Antenna Configurations for the MMA

Tamara T. Helfer & M.A. Holdaway
Last changed 11/11/98

Revision History:
11/11/98: Added summary and milestone tables. Added chapter number to section numbers, tables and figures.

Summary

Design concepts and sample layouts for antenna configurations for the MMA are presented.

Table 15.1 Guidelines for Configuration Design

Main D&D Task	Design a set of configurations which allow for a range of angular resolution and sensitivity
Flexible design philosophy	Configurations must allow for graceful expansion through possible collaboration
Costing	Optimize for shared stations to minimize cost
Site placement	Choose specific locations for antenna placement on Chajnantor site

Table 15.2 Principal milestones for configuration design during D&D Phase

"Donut" design philosophy accepted by MDC Working Group	9/14/98
Results of imaging simulations to test strawperson configurations	6/99
Present specific locations for antenna placement that take into account site characteristics	9/99
Present imaging simulations to test specific configurations	2/00
Preliminary Design Review	3/01/00

15.1 Number and Size of Antenna Elements

We assume that the MMA will comprise N = 36 antennas of 10 m diameter. The geometric collecting area is then 2830 sq. m; the ‘‘collecting length’’ nD, the appropriate measure of the mosaicing sensitivity and for the fraction of occupied cells, is 360 m. Both the collecting area and collecting length are superior to

the old MMA plan with N = 40 and D = 8 m. We note that the array configuration development plan will need to react to the changes and refinements in the array's concept, particularly with regard to possible collaboration with European and/or Japanese partners.

15.2 Limiting Configurations, Number of Configurations, and Resolution Scale Factor

15.2.1 Size of the Most Compact Array

The choice of a compact configuration for the MMA is driven by the desire to maximize surface brightness sensitivity, which is achieved by placing the antennas as close together as is practical. If we assume a filling factor f_{min} of 40%, which is a reasonable compromise between the competing requirements of close packing and the resultant maximum acceptable sidelobes, then the maximum baseline for the compact array is $b_{compact} = D_a\sqrt{N_a / f_{min}}$ = 95 +/- 5 m. This array would have the same resolution as a ring array that is about 66 +/- 4 m in diameter.

15.2.2 Size of the Largest Array

The largest configuration is assumed to have a maximum baseline of 3 km. If the sensitivity of the MMA is significantly expanded through a collaboration with the European and/or Japanese groups, then an array of 10 km diameter will be an attractive possibility.

15.2.3 Number of Configurations and Resolution Scale Factor

Given the assumed sizes of the minimum and maximum arrays, Holdaway (1998a) has performed a cost-benefit analysis for the number of MMA configurations, which showed that the observing efficiency of the MMA would be close to optimal with 4 configurations. We assign these four arrays the letters A (for the largest) through D (for the most compact). Given the described sizes of the D and A arrays, the resolution scale factor between adjacent configurations is about 3.6, and the configuration diameters are 95 m, 240 m, 840 m, and 3000 m. The minimum and maximum baselines for each array are listed in Table 15.3, along with the size of a sample beam and the time required for the half of the (u,v) cells to be sampled (FOC = 0.5). We note that the shortest baseline does not correspond to the largest angular structure to which the array will be sensitive, as mosaicing with total power data will permit arbitrarily large sources to be imaged.

Array	Minimum Baseline [m]	Maximum Baseline [m]	Array Style	Time for FOC = 0.5 [hours]	Natural Beam at 1 mm [arcs]
A	20	3000	?	10	0.06
B	18	840	?	2	0.20
C	16	240	?	0.1	0.75
D	12.8	95	filled	0	2.7 **Table 15.3** Approximate specifications for the MMA's four main configurations.

Table 15.3 Approximate specifications for the MMA's four main configurations.

15.3 Fourier Plane Coverage

The D and C arrays will provide essentially complete sampling of the (u,v) plane in a snapshot observation. The B and A arrays will require longer tracks for good imaging and sensitivity.

15.3.1 D Array

The driving considerations for the D array are maximum surface brightness sensitivity and excellent mosaicing capability. Surface brightness sensitivity is optimized by designing an array with the largest synthesized beam possible, which is achieved by having the shortest baselines possible. The MMA will be a *homogeneous array*, with total power and interferometric data being collected by the same antennas (Cornwell, Holdaway, and Uson, 1994). Homogeneous array mosaicing image quality is optimized by having a high density of the shortest interferometric baselines and by minimizing the sidelobes in the synthesized beam. Optimizing the short baseline coverage is best achieved with a filled array, which produces a Fourier plane coverage that to first order is a linearly decreasing function of (u,v) distance. The shortest baselines are limited strictly by the minimum safe distance which avoids mechanical collision of the antennas when pointing in arbitrary directions, which depends upon the antenna design, and less strictly by shadowing requirements. Configurations with the highest density of the shortest baselines will be a hexagonal close pack distribution of antennas, which results in a very large grating response in the synthesized beam and is therefore not acceptable. With a minimum distance between antennas of 1.28 D, we can achieve a reasonable sidelobe level of a few percent rms with an array filling factor of 40%. Such a filled compact array will result in complete instantaneous (u,v) coverage, even with only 32 antennas. Some degree of optimization is required for the zenith D array, trading off between good short baseline coverage and a large beam on the one hand and minimum synthesized beam sidelobes on the other.

15.3.1.1 D1, D2, and D3 Arrays For Observing Sources at Different Declinations

Since the beam shape will change with declination, it is always nice to have multiple configurations which are optimized to give circular beam shapes for both low elevation and zenith observations. However, the short spacing requirement for homogeneous array mosaicing, together with the physical inevitability of shadowing, absolutely require multiple compact configurations for observations of sources at various declinations. Current plans call for three compact arrays. The D1 array, with a North-South elongation of 1.2, will cover zenith observations down to somewhat below the onset of shadowing at 50 deg; the D2 and D3 will be progressively more elongated, with elongations of about 1.6 and 3. These three arrays will

cover most of the range of declinations available from the Chajnantor site, -90 deg $< \delta <$ 53 deg.

Observations of the small fraction of the sky which is further north and still visible from Chajnantor will need to be conducted in the C array or in a hybrid D+C configuration.

The D1 and D2 configurations will utilize a mechanical elevation stop which will limit the elevation to be above 20 deg. This limitation will permit a closer packing of the antennas in the D1 and D2 configurations. While it does remove flexibility from the compact arrays, the D1 and D2 arrays would be largely shadowed below this elevation anyway. The elevation stop will be removed from all or most antennas when they are reconfigured into the D3 array, where the antennas will be sufficiently separated that collisions are no longer a possibility. The general specifications for the D1, D2, and D3 configurations are shown in Table 15.4.

Array	Minimum N-S Distance	Elevation of first Shadowing	Minimum Observing Elevation	Maximum Observing Elevation	N-S Array Elongation
D1	1.3 D	50 deg	40-45	90	1.2
D2	1.9 D	31 deg	30	50+	1.6
D3	3.0 D	19 deg	14	33+	2.9 **Table 15.4** Specifications for the three D configurations. Configurations D1 and D2 will have a mechanical minimum elevation limit of 20 deg.

Table 15.4 Specifications for the three D configurations. Configurations D1 and D2 will have a mechanical minimum elevation limit of 20 deg.

We plan to optimize the three D configurations to allow for overlapping stations. The minimization of antenna stations may be important in keeping down the cost of building the pads, roads, and cables, though we still need to investigate what these costs are. Overlapping the stations will also keep the time involved in reconfiguring the antennas to a minimum. Also, we will need to design each D configuration with antenna access in mind: we should maximize the number of antennas that can be moved by a transporter without moving any other antennas.

15.3.2 C, B, and A Arrays

The C array will often be used for mosaicing, as the C array will have almost complete instantaneous (u,v) coverage, will have good brightness sensitivity, and will have an abundance of short baselines. Since long tracks are never needed to fill out the (u,v) coverage in C array, but rather to increase sensitivity, it will usually be better to observe a source within a few hours of transit to minimize the decrease in sensitivity caused by the atmospheric opacity at low elevations, and to observe over several days if more sensitivity is required (Holdaway, 1998b). Hence, the C array should be optimized for short tracks observed within a few hours of transit, over a range of declinations.

The B array requires about 2 hours to achieve essentially complete (u,v) coverage (FOC = 0.5, see Table 15.4), so it should be optimized for somewhat longer tracks, but still within a few hours of transit (Holdaway, 1998b).

The A array requires about 10 hours to achieve essentially complete (u,v) coverage. At +/- 5 hours off transit, the sensitivity loss due to the atmosphere will be severe at most frequencies; also, some sources are not above the minimum elevation limit for such long tracks. Nonetheless, the A array should be

optimized for long integrations, keeping in mind that it must also have respectable snapshot coverage for those sources strong enough to be observed in this mode.

As a general requirement, we will want to have some of the shortest baselines (i.e., 15-20 m) present in even the largest arrays to permit single configuration mapping of many wide field objects (Braun, 1993). However, if there is a lot of large structure in the object, multiple configuration imaging may be required. At this point, we do not have a coherent strategy for when to combine data from multiple configurations, nor have we considered the impact of multiple configuration observations on the set of configuration designs.

Two philosophies are currently under consideration for the Fourier plane coverage for the C, B, and A array configurations. One philosophy is to achieve as uniform coverage in the Fourier plane as is practical; this approach leads to ringlike arrays, as characterized by Keto (1997) for snapshot observations and by Holdaway, Foster & Morita (1996) for longer tracks. The other philosophy is to minimize the sidelobes in the synthesized beam, as implemented by Kogan (1997, 1998a).

15.3.2.1 The Keto Approach

Keto's Releaux triangle configurations, and ring-like configurations in general, yield fairly uniform (u,v) coverage plus a narrow peak at small spatial frequencies. They also offer the advantage of achieving the maximal sensitivity for the longest baselines, resulting in smaller naturally weighted resolution than other types of arrays with the same maximum baseline, which is an attractive characteristic especially for the A array.

However, true uniform coverage in the Fourier plane has disadvantages as well:

- the sharp cutoff in (u,v) sampling at large spatial frequencies results in large (10-15%) sidelobes close to the central lobe of the synthesized beam (Holdaway 1997), which may complicate an image deconvolution and thereby lower its dynamic range (Holdaway 1996).
- optimization techniques like the elastic net method used by Keto have so far tended to produce large diameters for the central hole in the Fourier plane coverage. It is probable that this problem can be alleviated to some extent, either by using nested rings or Releaux triangles, or by changing the optimization conditions to include some number of short baselines. The nested triangle approach destroys the uniform Fourier plane coverage.
- unpublished simulations by Morita and by Holdaway show that the excess short spacing coverage which a ring array provides is actually more responsible for high dynamic range in wide-field reconstructions than the uniform Fourier plane coverage. In other words, even if it were possible to get perfectly uniform Fourier plane coverage with a 36 element array, we probably would not want it.

15.3.2.2 The Kogan Approach

Kogan's algorithm produces antenna configurations which minimize the maximum sidelobe levels of the point spread function in some region of the image plane. This approach has the advantage of producing PSFs which should introduce fewer problems in image deconvolution. Kogan has also pointed out that in general, sidelobes that are close to the peak of the PSF can be alleviated using a taper (at the expense of image sensitivity), but that this is not true for sidelobes further out in the image plane. Another attractive feature of Kogan's approach is that it naturally shrinks the hole in the center of the (u,v) plane as the

optimization extends over larger and larger regions in the image plane. This produces good coverage at short baselines in the (u,v) plane, which is one of the main shortcomings of the uniform (u,v) coverage optimization described above.

Kogan's code is flexible and can accept a variety of topographical constraints as inputs. At this writing, Kogan is investigating the arrays produced when the antennas are distributed within an annulus with a fixed outer radius and with varying inner radii. With a ''donut'' array like this, this configuration can deviate enough from a ring to taper the beam naturally, thereby reducing its sidelobes. We are currently trying to optimize the width of the donut constraint for the various different arrays. Our best guess is that it will be desirable for the C array to be a rather filled configuration (i.e. with a thick annulus), and that the A array will be much more ringlike, to meet the differing requirements of these arrays as outlined above.

The Kogan arrays are optimized for a snapshot in the zenith direction only; however, changing the declination should change only the positions and not the amplitudes of the sidelobes for a snapshot observation (Kogan 1998a). It should be noted that an array which has optimal sidelobes for a snapshot at transit may not be optimal for long tracks.

One disadvantage to Kogan's approach of minimizing the maximum sidelobe within some region of the points spread function is that rather large sidelobes can lurk just outside the region of optimization. It might be better to extend the region of optimization to the full width of the primary beam, and apply a weighting function which emphasizes the minimization of the close in sidelobes and gradually relaxes for the very far out sidelobes.

We plan to study the ramifications of these competing philosophies and ultimately to select a design based on imaging simulations of sources of different size and structure.

15.4 Sample Configurations

Since the configuration optimization is still in progress, we do not attempt to present optimized configurations in this document. However, to give the reader a feel for the arrays that the Keto and Kogan algorithms produce, we present sample configurations in Figures 15.1 through 15.4.

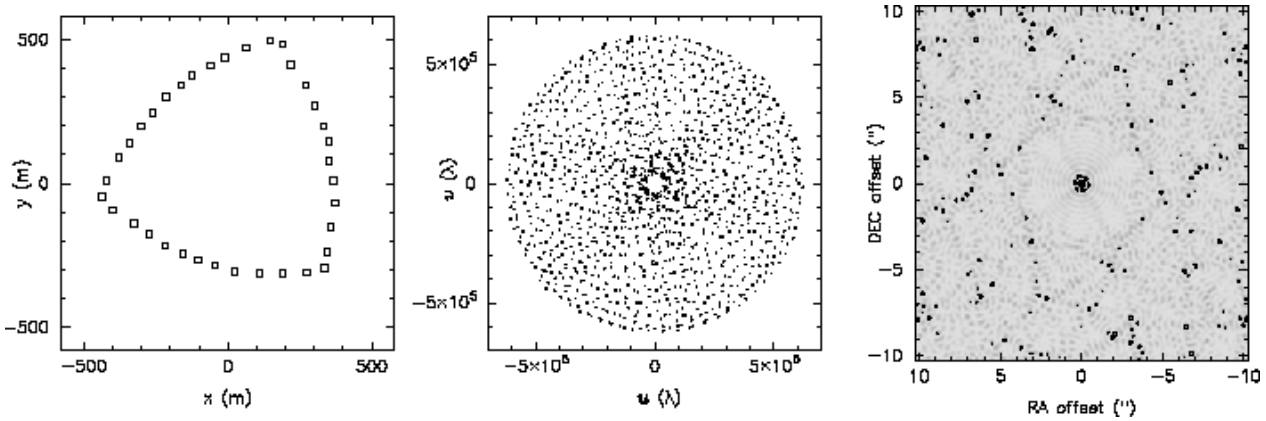

Figure 15.1: Sample Keto B Array snapshot at 230 GHz. (*left*) Antenna locations in meters, (*middle*) snapshot (u,v) converage, and (*right*) the resulting synthesized beam, with contours are at 10, 20, 40, 60,

80, 100%. Note the large inner sidelobes.

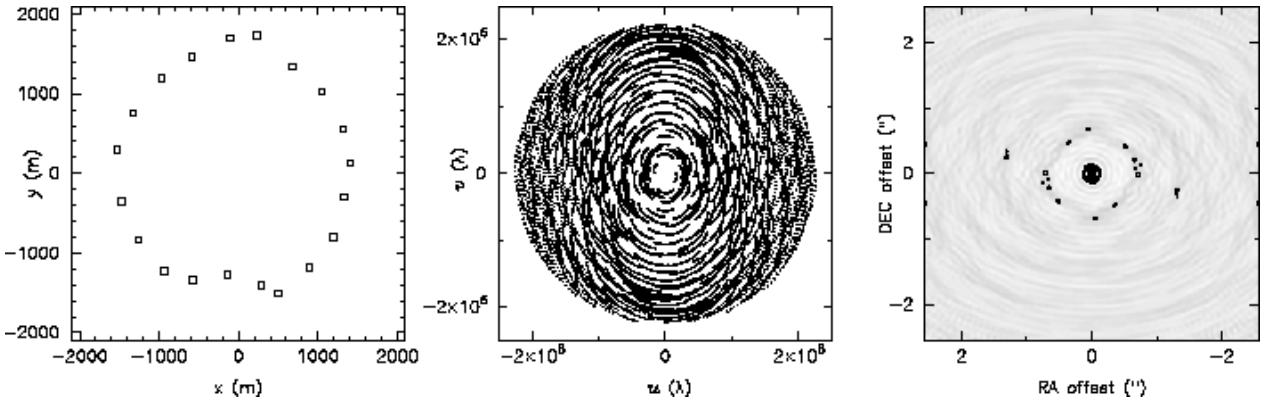

Figure 15.2: Sample A Array track for a Keto 20-element array optimized for 4-hour tracks (Holdaway, Foster, & Morita 1996), at 230 GHz. The contours are 0.05, 0.10, 0.15, 0.20, 0.40, 0.60, 0.80, 1.0. The outer sidelobes are reduced for long tracks, but the inner sidelobes remain high.

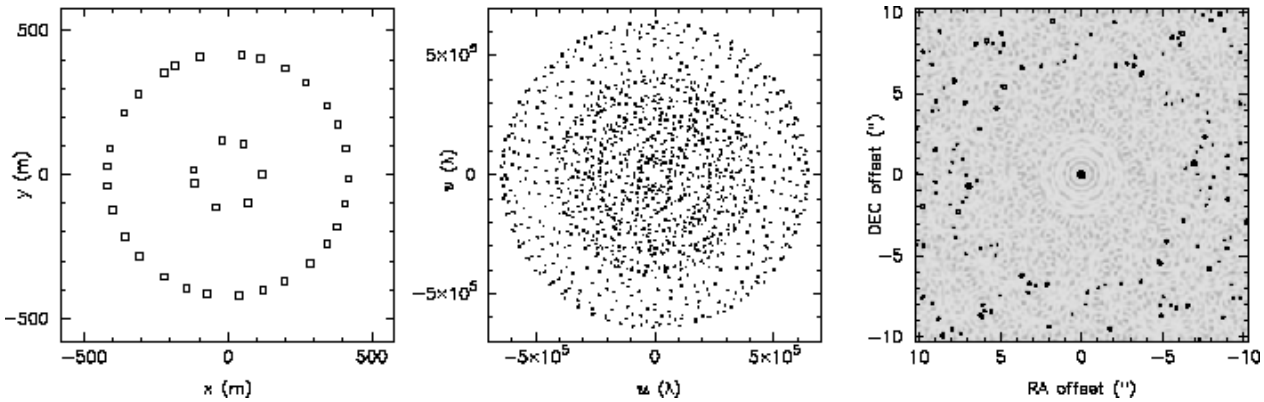

Figure 15.3: Sample Kogan B Array at 230 GHz. The contours are 10, 20, 40, 60, 80, 100%. The region of the image plane which was specified for the sidelobe minimization is a circular region at about 6" in radius.

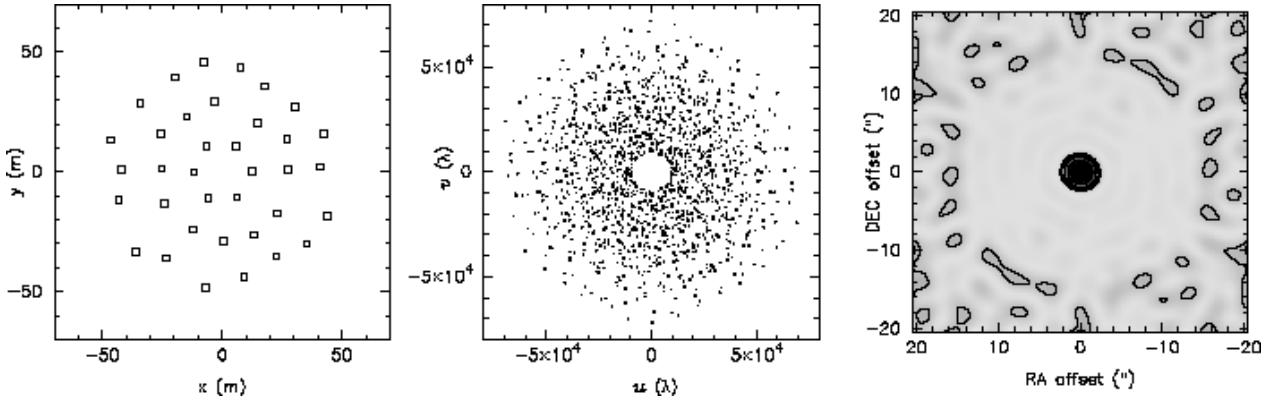

Figure 15.4: Sample zenith D array at 230 GHz. Except for the central hole, the Fourier plane density decreases nicely with (u,v) radius. This results in a synthesized beam with low sidelobes, shown here as 5, 10, 20, 40, 60, 80, 100% contours. Note that the primary beam of a 10 m antenna is about 30 FWHM at 230 GHz, so that the sidelobes are below 5% over essentially the entire primary beam.

15.5 Hybrid Arrays and Optimal Elongation for C, B, and A Arrays

From a study of the deviation of synthesized beams from circular as a function of source declination, Foster (1994) concluded that the optimal North-South elongation for tracks of varying length was in the range 1.1-1.3. In order to optimize the elongations of all of the arrays, it is important to know the expected source distribution with declination. Holdaway et al. (1996) assumed a model source distribution in order to estimate the pointing errors for the MMA antenna design. We are now in the process of looking at IRAS source distribution with declination in order to get a better estimate of this function.

Hybrid arrays, made by using stations in adjacent configurations, can be used to help minimize the shadowing and to achieve more circular beams for low-elevation sources. As stated above, a set of hybrid arrays is absolutely required for the compact configurations, but not so crucial for the larger arrays. Hybrid arrays will be studied more in the future when the basic arrays are better determined.

15.6 Interfaces With Other Parts of the MMA Project

- Antenna: minimum distance for close packing, hard elevation stops
- Antenna: transporter issues, such as intervening antenna clearance, road grade, etc.
- Site Development and Antenna: Antenna Pad Design.
- Site Development: Road Design.
- Local Oscillator/System: underground cables.

15.7 Other issues to be addressed

There are certainly other issues which have not been examined in this document which deserve closer attention. For example, all of the arrays will need to be optimized with respect to the Chajnantor site; the basic constraints of the site topography have already been implemented in both the Keto and Kogan

algorithms. The arrays will also need to be optimized for different source declinations, or simultaneously for multiple declinations.

The configuration design process has been evolving rapidly in the past few months. In the month since the original draft of this chapter was written, four new MMA Memos have been submitted. Kogan (1998b) has described his optimization using ‘‘donut’’ constraints described briefly here in Section 3.2.2. Webster (1998) has investigated the idea of using nested rings or nested Reuleaux triangles to achieve a compromise between uniform (u,v) coverage and sensitivity to extended structure. Conway (1998) has explored a novel approach of having configurations laid out using a logarithmic spiral geometry. Finally, Kogan (1998c) has explored the possibility of constraining antennas to lie on two circles such that the inner circle of the A array is the same as the outer circle of the B configuration, the inner circle of the B array is the same as the outer circle of the C configuration, and so forth. We defer further discussion and analysis of these works to a future version of this document.

References

Braun, R., 1993, ‘‘Telescope Placement at the VLA for Better Single Configuration Imaging’’, VLA Scientific Memo 165.

Conway, J., 1998, ‘‘Self-Similar Spiral Geometries for the LSA/MMA’’, MMA Memo #216.

Cornwell, Holdaway, and Uson, 1994, ‘‘Radio-interferometric imaging of very large objects: implications for array design’’, A&A 271, 697-713.

Foster, S.M. 1994, ‘‘The Optimum Elongation of the MMA A Configuration’’, MMA Memo #119

Holdaway, M.A., 1998a, ‘‘Cost-Benefit Analysis for the Number of MMA Configurations’’, MMA Memo #199

Holdaway, M.A., 1998b, ‘‘Hour Angle Ranges for Configuration Optimization’’, MMA Memo #201

Holdaway, M.A., 1997, ‘‘Comments on Minimum Sidelobe Configurations’’, MMA Memo #172

Holdaway, M.A., 1996, ‘‘What Fourier Plane Coverage is Right for the MMA?’’, MMA Memo #156

Holdaway, M.A., Foster, S.M., Emerson, D., Cheng, J., & Schwab, F. 1996, ‘‘Wind Velocities at the Chajnantor and Mauna Kea Sites and the Effect on MMA Pointing’’, MMA Memo # 159

Holdaway, M.A., Foster, S.M., & Morita, K.-I. 1996, ‘‘Fitting a 12 km Configuration on the Chajnantor Site’’, MMA Memo #153

Keto, E. 1997, ‘‘The Shape of Cross-correlation Interferometers’’, ApJ, 475, 843

Kogan, L. 1997, ‘‘Optimization of an Array Configuration Minimizing Side Lobes’’, MMA Memo # 171

Kogan, L. 1998a, ‘‘Opimization of an Array Configuration with a Topography Constraint’’, MMA Memo #202

Kogan, L. 1998b, ‘‘Opimization of an Array Configuration with a Donut Constraint’’, MMA Memo #212

Kogan, L. 1998c, ‘‘A, B, C, and D Configurations in the Shape of Concentric Circles’’, MMA Memo #217.

Webster, A. 1998, ‘‘Hybrid Arrays: The Design of Reconfigurable Aperture-Synthesis Interferometers’’, MMA Memo #214.